



Published in final edited form as:

J Orthop Res. 2008 October ; 26(10): 1340–1346. doi:10.1002/jor.20620.

Differential effects of biologic vs bisphosphonate inhibition of wear debris-induced osteolysis assessed by longitudinal micro-CT

Ryosuke Tsutsumi^{1,2}, Colleen Hock¹, C. Dustin Bechtold¹, Steven T. Proulx¹, Susan V. Bukata¹, Hiromu Ito², Hani Awad¹, Takashi Nakamura², Regis J. O'Keefe¹, and Edward M. Schwarz^{1,3}

¹The Center for Musculoskeletal Research, University of Rochester, Rochester, New York

²Department of Orthopaedic Surgery, Kyoto University Medical School, 54 Kawahara-cho, Shogoin, Sakyo, Kyoto 606–8507, Japan

Summary

Aseptic loosening secondary to periprosthetic osteolysis remains a serious orthopaedic problem and the greatest limitation of total joint replacement. This process is caused by wear debris-induced osteoclastic bone resorption, for which effective small molecule (bisphosphonates, BPs) and biologic (RANK antagonists) drugs have been developed. While BPs have proven to be effective in preventing metabolic bone loss in non-inflammatory conditions such as osteoporosis, they do not have the same efficacy in the setting of inflammatory bone loss such as that observed in periprosthetic osteolysis. Since this difference has been attributed to the anti-apoptotic inflammatory signals that protect osteoclasts from BP-induced apoptosis, but not RANK antagonists, we tested the hypothesis that osteoprotegerin (OPG) is more effective in preventing wear debris-induced osteolysis than zoledronic acid (ZA) or alendronate (Aln) in the murine calvaria model. Based on the shortcomings of previous animal studies that focused on 2D imaging and histology endpoints, and the emergence of quantitative 3D-CT, we developed *in vivo* micro-CT methods for the murine calvaria model to more rigorously test our hypothesis and correlate the osteolysis results with traditional histology. Although this approach proved to be incompatible with titanium (Ti) particles, due to metal artifact, we were able to demonstrate a 3.2-fold increase in osteolytic volume over 10 days induced by ultra high molecular weight polyethylene (PE) particles vs. sham controls (0.49 ± 0.23mm³ vs. 0.15 ± 0.067mm³; *p*<0.01). While OPG and high dose ZA completely inhibited this PE-induced osteolysis (*p*<0.001), pharmacological doses of ZA and Aln were less effective but still reached statistical significance (*p*<0.05). Traditional histomorphometry of the sagittal suture area of calvaria from both Ti and PE treated mice confirmed the remarkable suppression of resorption by OPG (*p*<0.001) vs. the lack of effect by physiological BPs. The differences in drug effects on osteolysis were largely explained by the significant difference in osteoclast numbers observed between OPG vs. BPs in both Ti and PE treated calvaria; and linear regression analyses that demonstrated a highly significant correlation between osteolysis volume and sagittal suture area vs. osteoclast numbers (*p*<0.001). Taken together our results demonstrate the sensitivity and utility of *in vivo* 3D-CT to detect the effects of BPs on wear debris-induced osteolysis that could not be observed by histology alone; and that the greater suppression of bone resorption observed with OPG treatment vs. BPs is due to its ability to dramatically reduce osteoclast numbers in the presence of inflammatory signals.

³To whom correspondence should be addressed: Dr. Edward M. Schwarz The Center for Musculoskeletal Research University of Rochester Medical Center 601 Elmwood Avenue, Box 665, Rochester, NY 14642 Phone 585–275–3063, FAX 585–756–4727 E-mail: Edward_Schwarz@URMC.Rochester.edu..

Keywords

Aseptic Loosening; wear debris; osteolysis; osteoprotegerin (OPG); bisphosphonate (BP); 3D-micro-CT

Introduction

Although total joint replacement (TJR) is one of the most successful surgeries in all of medicine, with more than 1 million being performed each year,¹ its long-term results are limited by periprosthetic osteolysis and subsequent aseptic loosening in approximately 20% of patients.² It has long been established that this process is caused by the generation of implant wear debris that stimulates an inflammatory response and osteoclastic resorption at the bone-implant interface, and the subject has recently been reviewed.¹ Thus, it has been proposed that drugs that inhibit the osteoclast should be effective in preventing aseptic loosening.³

Two distinct classes of drugs that specifically target the osteoclast have been developed, bisphosphonates (BPs) and nuclear factor kappa B ligand (RANKL) antagonists.^{4,5} While BPs have been widely used as anti-resorptive agents for various metabolic bone diseases (e.g. osteoporosis, Paget's disease, bone cancer),⁶ they have not demonstrated clinical efficacy in the setting of inflammatory bone loss such as rheumatoid arthritis (RA).⁷⁻¹¹ This lack of efficacy has been attributed to inflammation-derived anti-apoptotic signals, such as tumor necrosis factor (TNF) induced Bcl-Xl gene expression that protect osteoclasts from BP-induced apoptosis.¹² In contrast, RANK signaling has been demonstrated to be essential for osteoclast formation in response to both remodeling and inflammatory signals, as RANK deficient mice have no osteoclasts¹³ and do not form them in response to TNF¹⁴ or wear debris-induced inflammation.¹⁵ Given these apparent differential effects of BPs and RANKL antagonists on osteoclast apoptosis in the setting of inflammatory bone loss, here we aimed to test the hypothesis that osteoprotegerin (OPG) is more effective in preventing wear debris-induced osteolysis than zoledronic acid (ZA) or alendronate (Aln).

While various animal models have been developed to study the pathogenesis of aseptic loosening, none of them can faithfully recapitulate the biological, biomechanical and mechanical factors that contribute to the clinical situation.¹ Thus, many investigators whose research is focused on the biology of wear debris-induced osteolysis have found the murine calvaria model to be particularly useful due to its cost efficiency and the ability to incorporate genetically defined strains to test molecular hypotheses¹⁶⁻¹⁸. However, until now the quantitation of osteolysis in this model has been limited to cross-sectional 2D histology and plain x-rays. Given the translational importance of quantitative 3D longitudinal imaging,^{19,20} and the emergence of *in vivo* micro-CT imaging as the most sensitive outcome measure of bone volume,²¹ here we aimed to develop this approach for the murine calvaria model. In so doing, we also tested the hypothesis that volumetric micro-CT is more sensitive than 2D histology for quantifying the differences between BP and biologic therapy of wear debris-induced osteolysis.

Methods

Particles

Pure titanium (Ti) particles were obtained from Johnson Mathey Chemicals (Ward Hill, MA, USA), and resuspended in phosphate-buffered saline (PBS) at a concentration of 1×10^8 particles/ml as previously described.²² More than 90% of the Ti particles were determined to be $<5 \mu\text{m}$ in diameter by Coulter Channelizer analysis. The UHMWPE (PE) particles (Ceridust 130), were obtained as a gift from Dr. E. M. Greenfield, and were prepared as previously

described.¹⁸ The mean size of the particles was 7.1 μm in diameter, and approximately 75% of the particles were less than 9.1 μm in diameter as determined by Coulter counter analysis.¹⁸ Due to technical difficulties in quantifying submicron particles and their biological effects that are distinct from submicron particulate aggregates, the proportion of submicron particles in the Ti and PE wear debris was not determined. A Limulus assay (BioWhittaker, Walkersville, MD, USA) was used to ensure that both Ti and PE particles were free of endotoxin.

Animal surgery and drug treatment

All animal studies were performed under University of Rochester Committee for Animal Resources approved protocols. The *in vivo* mouse calvaria experiments were performed as previously described.²² Briefly, eight healthy female 8-week-old C57BL/6 mice were used in each group. Mice were anesthetized with 70–80 mg/kg of ketamine and 5–7 mg/kg of xylazine by intraperitoneal (i.p.) injection. A 0.5 cm × 0.5 cm area of calvarial bone was exposed by making a midline sagittal incision over the calvaria, leaving the periosteum intact. No particles (sham surgery), 20 mg Ti particles, or 5 mg PE particles were spread over the area and the incision was closed with sutures. A single intraperitoneal (i.p.) injection of PBS was performed (placebo). For drug treatments, we chose to study OPG and ZA based on pre-clinical and clinical testing that has determined that are the most potent drugs in their respective class^{4,5} We also studied Aln since it is to most commonly prescribed BP. For drug administration, we used 5 mg/kg of OPG (Amgen Inc, Thousand Oaks, CA)²³ and 0.1 mg/kg ZA (Amgen Inc, Thousand Oaks, CA),²⁴ based on safety and efficacy clinical trials that have determined these levels to be the maximal pharmacological doses in a single injection, and their successful use in the mouse calvaria model of wear debris-induced osteolysis.^{25,26} Although its toxic profile is unfit for human use, we also tested high dose ZA (0.15 mg/kg) based on murine arthritis studies that have demonstrated its ability to prevent focal erosions.²⁷ These drugs were administered to the mice three days after surgery as previously described²⁸. Intermittent intraperitoneal (i.p.) injections of Aln (10 μg/kg, Calbiochem, San Diego, CA) were administered to a separate group of mice 3, 6 and 9 days after surgery as previously described.²²

In vivo micro-CT imaging and volumetric osteolysis analysis

High resolution *in vivo* micro computed tomography (VivaCT40, ScanCo Medical Basserdorf Switzerland) of calvarial bone structure was performed on day 0 (before surgery) and day 10 (after surgery). The mice were anesthetized with 2% isofluorine and 1 L/min oxygen. The skulls were scanned with isometric resolution of 35.8 μm. The X-ray source was set at a voltage of 45 kV and a current of 155 μA using an integration time of 300 msec. Mice were scanned for 33.3 minutes with an average of 528 slices. The Viva CT40 software was used to create DICOM files, which were transferred to Amira 3.1 (TGS, Mercury Computer Systems, Inc., San Diego, CA) for quantitative analysis. Quantification of the osteolytic volume was performed by subtracting a registered 3D day 10 image from its baseline counter part in Amira 3.1 as follows. The protocol for registration of calvaria at different time points and quantification of erosion in Amira 3.1 from microCT data is as follows. First, the DICOM images from day 0 and day 10 calvaria were imported into Amira 3.1 with an automatic registration module (Optimizer: LineSearch; Optimizer step: initial: 0.336 and final: 0.0001; Metric: Euclidean). Then the Arithmetic module was used to subtract the registered day 10 image from the day 0 image. Next, a region of interest defined by the operator as the largest osteolytic volume that fits in a 125×125×125 voxel template (89.6 mm³) on the subtracted image was manually isolated using the Crop Editor. Within this sectioned volume, the Segmentation Editor was used to “label” all voxels over a gray scale threshold value of 5,000 (arbitrary units) as bone. Finally, the TissueStatistics module then converted this positive volume to the osteolytic volume of the sample.

Histologic evaluation of osteolysis and osteoclast numbers

Ten days after surgery the mice were sacrificed and the calvaria were harvested for decalcified histology as previously described²⁹. Osteolysis was quantified from three contiguous 3 μm sections 500 μm apart, stained with orange/G by measuring the soft tissue space between the parietal bones (Sagittal Suture Area, SSA) as previously described²², using ScionImage software (Scion Corporation, Frederick, MD, USA). Osteoclasts were quantified as previously described²²; using three contiguous 3 μm sections 500 μm apart, which were stained for tartrate-resistant acid phosphatase (TRAP) using the Diagnostics Acid Phosphatase Kit (Sigma, St. Louis, MO, USA).

Statistical analysis

All values are presented as means \pm SD. Statistical significance was determined using a one-way ANOVA with multiple comparison of Tukey of six treatment groups where $p < 0.05$ was considered significant. Correlations between 3D and 2D osteolysis versus osteoclast number were estimated using Pearson's correlation coefficient and tested for significance using a two-sided t -test.

Results

Effects of OPG vs. ZA on Ti-induced osteolysis

Figure 1 shows the histology data from experiments in which we compared the effects of OPG and ZA on Ti-induced osteolysis. The results are consistent with our previous findings that RANK-ligand inhibition completely inhibits Ti-induced bone resorption and osteoclast formation.^{15,25} While the ZA treatment also inhibited osteolysis as previously described,²⁶ its effects were more variable and less significant (Figure 1A). TRAP staining for osteoclasts in these sections provides a clear explanation for these differential drug effects (Figure 1B). While most of the sections from OPG-treated mice were completely devoid of osteoclasts (Figure 1I), TRAP-stained sections from ZA treated mice were variable and contained evidence of active osteoclasts (Figure 1J, L) and apoptotic osteoclasts (Figure 1J, M). This finding supports our central hypothesis that BPs are ineffective at inducing osteoclast apoptosis in the setting of inflammatory bone loss such as wear debris-induced osteolysis.

To see if we could further distinguish the differences between OPG and BP therapy in our model by using a more sensitive outcome measure, we develop a longitudinal *in vivo* micro-CT approach that would quantify volumetric osteolysis directly rather than from 2D histology. Unfortunately, several attempts to subtract the Ti particles from the bone (Figure 2A) via threshold segmentation failed due to the similar density of the Ti and bone. This led us to conclude that rendering quantitative volumetric Ti-induced osteolysis in this model is not feasible. However, when we repeated these studies with radio transparent PE particles as previously described,¹⁸ we were able to clearly image 2D micro-CT slices of the calvaria without any particle interference (Figure 2A). This allowed for the volumetric quantification of osteolysis from an 89.6 mm³ region of interest (Figure 2B).

Having developed a volumetric micro-CT approach to quantify wear debris-induced osteolysis and the differential drug effects, we decided to include a high dose ZA group that has unacceptable side effects in humans, but has been successfully used to inhibit focal erosions in mice.²⁷ We also included an intermittent Aln group, since it has also been demonstrated to inhibit wear debris-induced osteolysis in murine²² and canine³⁰ models. The results of this volumetric osteolysis analysis are presented in Figure 3, which reveal several remarkable findings. First, 3D reconstruction of the calvaria demonstrated the significant 3.2-fold increase in volume of soft tissue between the parietal bones of PE-treated mice vs. sham surgery controls ($p < 0.01$). From the drug studies, it was clear that the OPG treatment completely inhibited the

PE-induced osteolysis, and perhaps normal bone remodeling as well, as very little soft tissue could be identified from the subtractive analysis. The high dose ZA treatment achieved a similar level of osteolysis inhibition compared to the OPG treatment ($p < 0.001$), however the results were more variable. In contrast, the low dose ZA and Aln groups demonstrated inferior inhibition, but still achieved statistically significant effects ($p < 0.05$).

Histomorphometry of the SSA (Figure 4A, C-F) and TRAP+ osteoclasts (Figure 4B, G-M) corroborated all of the findings in the Ti study in Figure 1. However, while this 2D approach was able to detect the highly significant effects of OPG vs. PBS ($p < 0.001$), it was not able to see any significant effects of the low dose ZA and Aln. Furthermore, while the high dose ZA significantly inhibited osteolysis ($p < 0.05$), these effects did not achieve the same level of significance as OPG treatment. Moreover, the data demonstrate the power of 3D micro-CT as a more sensitive measure of osteolysis inhibition compared to 2D histology based on its ability to distinguish significant differences between drug groups in a small pilot study.

Given that the differences in osteolysis appeared to closely resemble the differences in osteoclast numbers between the OPG and BP treatment groups, we performed a linear regression analysis with data for all of the drug treatment groups. Figure 5 demonstrates that osteolysis measured by both 3D micro-CT and 2D histomorphometry significantly ($p < 0.001$) correlates with osteoclast numbers in the calvaria. Moreover, osteoclast numbers alone can explain approximately 50% of the drug effects on osteolysis.

Discussion

Considering that the etiology of aseptic loosening has been largely understood for over 3 decades,³¹ and clinically proven anti-resorptive therapy has been available for millions of postmenopausal women with osteoporosis for over ten years,⁶ the absence of a therapeutic intervention for wear debris-induced osteolysis is very disappointing. The primary reason for this appears to be a fundamental difference between inflammatory vs. non-inflammatory bone loss, in which BPs appear to be effective only in non-inflammatory settings.⁷⁻¹¹

Previously, we have reported that osteoclasts obtain resistance to BP-induced apoptosis in the setting of inflammatory bone loss due to TNF upregulation of the anti-apoptosis factor Bcl-XI.¹² Since TNF is known to be expressed during wear debris-induced osteolysis,^{16,32} TNF is present at high levels in retrieved interfacial membranes,³³ and a polymorphism in the TNF gene promoter has been associated with aseptic loosening,³⁴ it is of interest to see if this mechanism of BP resistance applies to osteoclasts that mediate wear debris-induced osteolysis. Here we demonstrate that clinically relevant doses of BP are unable to significantly reduce osteoclast numbers in the murine calvaria model, and that this correlates with their inability to prevent wear debris-induced osteolysis. Remarkably, this is not the case for OPG treatment, which consistently eliminated osteoclasts and prevented both Ti and PE induced osteolysis. While this provides optimism that a RANKL antagonist like denosumab (Amgen, Thousand Oaks, CA), which is currently in phase 3 clinical trials,³⁵ might be an effective drug for aseptic loosening, the major limitations of this animal model need to be acknowledged. Specifically, the clinical condition involves osteolysis adjacent to a joint, which is exposed to continuous joint fluid pressure and newly generated wear debris particles. Another important clinical consideration is the duration of treatment, and potential side effects due to chronic osteoclast inhibition. However, many of these potential concerns will likely be addressed in the current phase 3 trials.

Acknowledgments

The authors would like to thank: Dr. Christopher Beck for biostatistical support, Laura Yanoso for technical assistance with the micro-CT, Krista Scorsone for technical assistance with the histology, and Kimberly Napoli for assistance in

preparing the manuscript. We would also like to thank Drs E.M. Greenfield for the PE particles and B.F. Boyce for interpretive analysis of the histology. This work was supported by unrestricted education grants from DePuy J&J and Amgen Inc., and National Institutes of Health PHS awards DE17096, AR46545, and AR54041.

References

1. Purdue PE, Koulouvaris P, Potter HG, Nestor BJ, Sculco TP. The cellular and molecular biology of periprosthetic osteolysis. *Clin Orthop Relat Res* 2007;454:251–61. [PubMed: 16980902]
2. Agarwal S. Osteolysis: basic science, incidence and diagnosis. *Curr Orthop* 2004;18:220–31.
3. Abu-Amer Y, Darwech I, Clohisey JC. Aseptic loosening of total joint replacements: mechanisms underlying osteolysis and potential therapies. *Arthritis Res Ther* 2007;9(Suppl 1):S6. [PubMed: 17634145]
4. Rodan GA, Martin TJ. Therapeutic approaches to bone diseases. *Science* 2000;289–5484:1508–14.
5. Boyle WJ, Simonet WS, Lacey DL. Osteoclast differentiation and activation. *Nature* 2003;423–6937:337–42.
6. Bone HG, Hosking D, Devogelaer JP, Tucci JR, Emkey RD, Tonino RP, Rodriguez-Portales JA, Downs RW, Gupta J, Santora AC, Liberman UA. Ten years' experience with alendronate for osteoporosis in postmenopausal women. *N Engl J Med* 2004;350–12:1189–99.
7. Ralston SH, Hacking L, Willocks L, Bruce F, Pitkeathly DA. Clinical, biochemical, and radiographic effects of aminohydroxypropylidene bisphosphonate treatment in rheumatoid arthritis. *Ann Rheum Dis* 1989;48–5:396–9.
8. Maccagno A, Di Giorgio E, Roldan EJ, Caballero LE, Perez Lloret A. Double blind radiological assessment of continuous oral pamidronic acid in patients with rheumatoid arthritis. *Scand J Rheumatol* 1994;23–4:211–4.
9. Eggelmeijer F, Papapoulos SE, van Paassen HC, Dijkmans BA, Valkema R, Westedt ML, Landman JO, Pauwels EK, Breedveld FC. Increased bone mass with pamidronate treatment in rheumatoid arthritis. Results of a three-year randomized, double-blind trial. *Arthritis Rheum* 1996;39–3:396–402.
10. Valleala H, Laasonen L, Koivula MK, Mandelin J, Friman C, Risteli J, Kontinen YT. Two year randomized controlled trial of etidronate in rheumatoid arthritis: changes in serum aminoterminal telopeptides correlate with radiographic progression of disease. *J Rheumatol* 2003;30–3:468–73.
11. Jarrett SJ, Conaghan PG, Sloan VS, Papanastasiou P, Ortmann CE, O'Connor PJ, Grainger AJ, Emery P. Preliminary evidence for a structural benefit of the new bisphosphonate zoledronic acid in early rheumatoid arthritis. *Arthritis Rheum* 2006;54–5:1410–4.
12. Zhang Q, Badell IR, Schwarz EM, Boulukos KE, Yao Z, Boyce BF, Xing L. Tumor necrosis factor prevents alendronate-induced osteoclast apoptosis in vivo by stimulating Bcl-xL expression through Ets-2. *Arthritis Rheum* 2005;52–9:2708–18.
13. Dougall WC, Glaccum M, Charrier K, Rohrbach K, Brasel K, De Smedt T, Daro E, Smith J, Tometsko ME, Maliszewski CR, Armstrong A, Shen V, Bain S, Cosman D, Anderson D, Morrissey PJ, Peschon JJ, Schuh J. RANK is essential for osteoclast and lymph node development. *Genes Dev* 1999;13–18:2412–24.
14. Li P, Schwarz EM, O'Keefe RJ, Ma L, Boyce BF, Xing L. RANK signaling is not required for TNFalpha-mediated increase in CD11(hi) osteoclast precursors but is essential for mature osteoclast formation in TNFalpha-mediated inflammatory arthritis. *J Bone Miner Res* 2004;19–2:207–13.
15. Childs LM, Paschalis EP, Xing L, Dougall WC, Anderson D, Boskey AL, Puzas JE, Rosier RN, O'Keefe RJ, Boyce BF, Schwarz EM. In vivo RANK signaling blockade using the receptor activator of NF-kappaB:Fc effectively prevents and ameliorates wear debris-induced osteolysis via osteoclast depletion without inhibiting osteogenesis. *J Bone Miner Res* 2002;17–2:192–9.
16. Merkel KD, Erdmann JM, McHugh KP, Abu-Amer Y, Ross FP, Teitelbaum SL. Tumor necrosis factor-alpha mediates orthopedic implant osteolysis. *Am J Pathol* 1999;154–1:203–10.
17. Zhang X, Morham SG, Langenback R, Young DA, Xing L, Boyce BF, Puzas JE, Rosier RN, O'Keefe RJ, Schwarz EM. Evidence for a Direct Role of COX-2 in Implant Wear Debris Induced Osteolysis. *J. Bon. Min. Res* 2001;16:660–70.
18. Taki N, Tatro JM, Nalepka JL, Togawa D, Goldberg VM, Rinnac CM, Greenfield EM. Polyethylene and titanium particles induce osteolysis by similar, lymphocyte-independent, mechanisms. *J Orthop Res* 2005;23–2:376–83.

19. Schwarz EM, Campbell D, Totterman S, Boyd A, O'Keefe RJ, Looney RJ. Use of volumetric computerized tomography as a primary outcome measure to evaluate drug efficacy in the prevention of peri-prosthetic osteolysis: a 1-year clinical pilot of etanercept vs. placebo. *J Orthop Res* 2003;21-6:1049-55.
20. Howie DW, Neale SD, Stamenkov R, McGee MA, Taylor DJ, Findlay DM. Progression of acetabular periprosthetic osteolytic lesions measured with computed tomography. *J Bone Joint Surg Am* 2007;89-8:1818-25.
21. Waarsing JH, Day JS, Weinans H. Longitudinal micro-CT scans to evaluate bone architecture. *J Musculoskelet Neuronal Interact* 2005;5-4:310-2.
22. Schwarz EM, Benz EB, Lu AL, Goater JJ, Mollano AV, Rosier RN, Puzas JE, O'Keefe RJ. A Quantitative Small Animal Surrogate To Evaluate Drug Efficacy in Preventing Wear Debris-Induced Osteolysis. *J. Ortho. Res* 2000;18:849-55.
23. Bekker PJ, Holloway D, Nakanishi A, Arrighi M, Leese PT, Dunstan CR. The effect of a single dose of osteoprotegerin in postmenopausal women. *J Bone Miner Res* 2001;16-2:348-60.
24. Carteni G, Bordonaro R, Giotta F, Lorusso V, Scalone S, Vinaccia V, Rondena R, Amadori D. Efficacy and safety of zoledronic acid in patients with breast cancer metastatic to bone: a multicenter clinical trial. *Oncologist* 2006;11-7:841-8.
25. Ulrich-Vinther M, Carmody EE, Goater JJ, Sb K, O'Keefe RJ, Schwarz EM. Recombinant adeno-associated virus-mediated osteoprotegerin gene therapy inhibits wear debris-induced osteolysis. *J Bone Joint Surg Am* 2002;84-A-8:1405-12. [PubMed: 12177271]
26. von Knoch M, Wedemeyer C, Pingsmann A, von Knoch F, Hilken G, Sprecher C, Henschke F, Barden B, Loer F. The decrease of particle-induced osteolysis after a single dose of bisphosphonate. *Biomaterials* 2005;26-14:1803-8.
27. Herrak P, Gortz B, Hayer S, Redlich K, Reiter E, Gasser J, Bergmeister H, Kollias G, Smolen JS, Schett G. Zoledronic acid protects against local and systemic bone loss in tumor necrosis factor-mediated arthritis. *Arthritis Rheum* 2004;50-7:2327-37.
28. Morony S, Warmington K, Adamu S, Asuncion F, Geng Z, Grisanti M, Tan HL, Capparelli C, Starnes C, Weimann B, Dunstan CR, Kostenuik PJ. The inhibition of RANKL causes greater suppression of bone resorption and hypercalcemia compared with bisphosphonates in two models of humoral hypercalcemia of malignancy. *Endocrinology* 2005;146-8:3235-43.
29. Ito H, Koefoed M, Tiyapatanaputi P, Gromov K, Goater JJ, Carmouche J, Zhang X, Rubery PT, Rabinowitz J, Samulski RJ, Nakamura T, Soballe K, O'Keefe R J, Boyce BF, Schwarz EM. Remodeling of cortical bone allografts mediated by adherent rAAV-RANKL and VEGF gene therapy. *Nat Med* 2005;11-3:291-7.
30. Shanbhag AS, Hasselman CT, Rubash HE. The John Charnley Award. Inhibition of wear debris mediated osteolysis in a canine total hip arthroplasty model. *Clin Orthop Relat Res* 1997;344:33-43. [PubMed: 9372756]
31. Willert HG. Reactions of the articular capsule to wear products of artificial joint prostheses. *J Biomed Mater Res* 1977;11-2:157-64.
32. Schwarz EM, Lu AP, Goater JJ, Benz EB, Kollias G, Rosier RN, Puzas JE, O'Keefe RJ. Tumor necrosis factor-alpha/nuclear transcription factor-kappaB signaling in periprosthetic osteolysis. *J Orthop Res* 2000;18-3:472-80.
33. Xu JW, Konttinen YT, Lassus J, Natah S, Ceponis A, Solovieva S, Aspenberg P, Santavirta S. Tumor necrosis factor-alpha (TNF-alpha) in loosening of total hip replacement (THR). *Clin Exp Rheumatol* 1996;14-6:643-8.
34. Wilkinson JM, Wilson AG, Stockley I, Scott IR, Macdonald DA, Hamer AJ, Duff GW, Eastell R. Variation in the TNF gene promoter and risk of osteolysis after total hip arthroplasty. *J Bone Miner Res* 2003;18-11:1995-2001.
35. Schwarz EM, Ritchlin CT. Clinical development of anti-RANKL therapy. *Arthritis Res Ther* 2007;9 (Suppl 1):S7. [PubMed: 17634146]

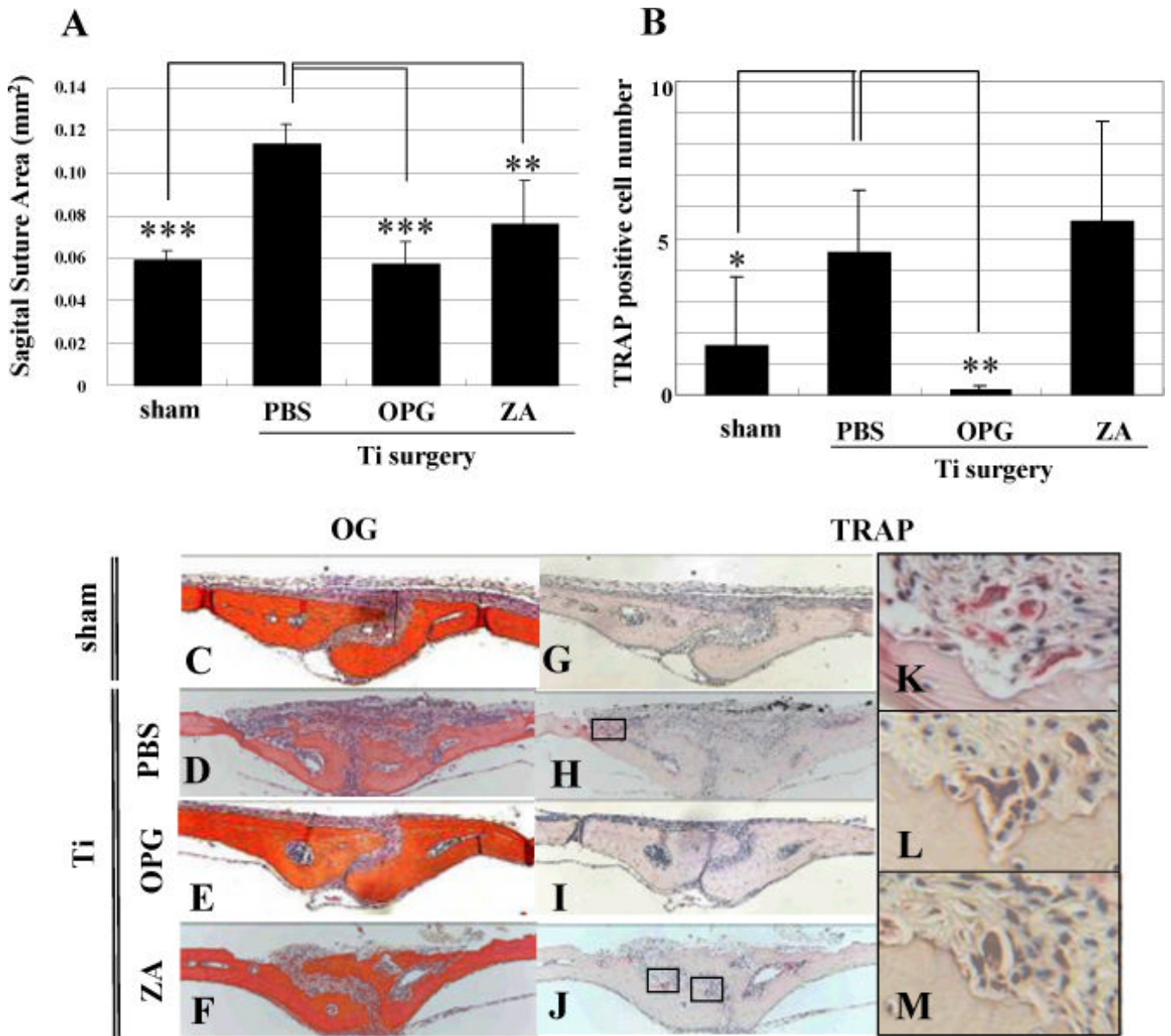


Figure 1. OPG vs. ZA inhibition of Ti-induced osteolysis
Mice (n=8) received sham or Ti surgeries to induce osteolysis over 10 days, and were given PBS, OPG or ZA (0.1mg/kg) treatment as indicated. Afterwards, calvaria were harvested for Orange/G and TRAP stained histology to quantify the SSA (A) and osteoclast numbers (B) as described in Materials and Methods. The data are presented as the mean \pm SD (* $p < 0.05$, ** $p < 0.01$, *** $p < 0.001$ vs. PBS control with Tukey test). Representative Orange/G (C-F) and TRAP (G-M) stained histology are presented at 100X (C-J). High power images of the boxed regions in H and J are also shown at 400X (K-M). Of note are the large number of active osteoclasts in the PBS group (H & K), the complete absence of osteoclasts in the OPG group (I) and the presence of both active (L) and apoptotic (M) osteoclasts in the ZA groups.

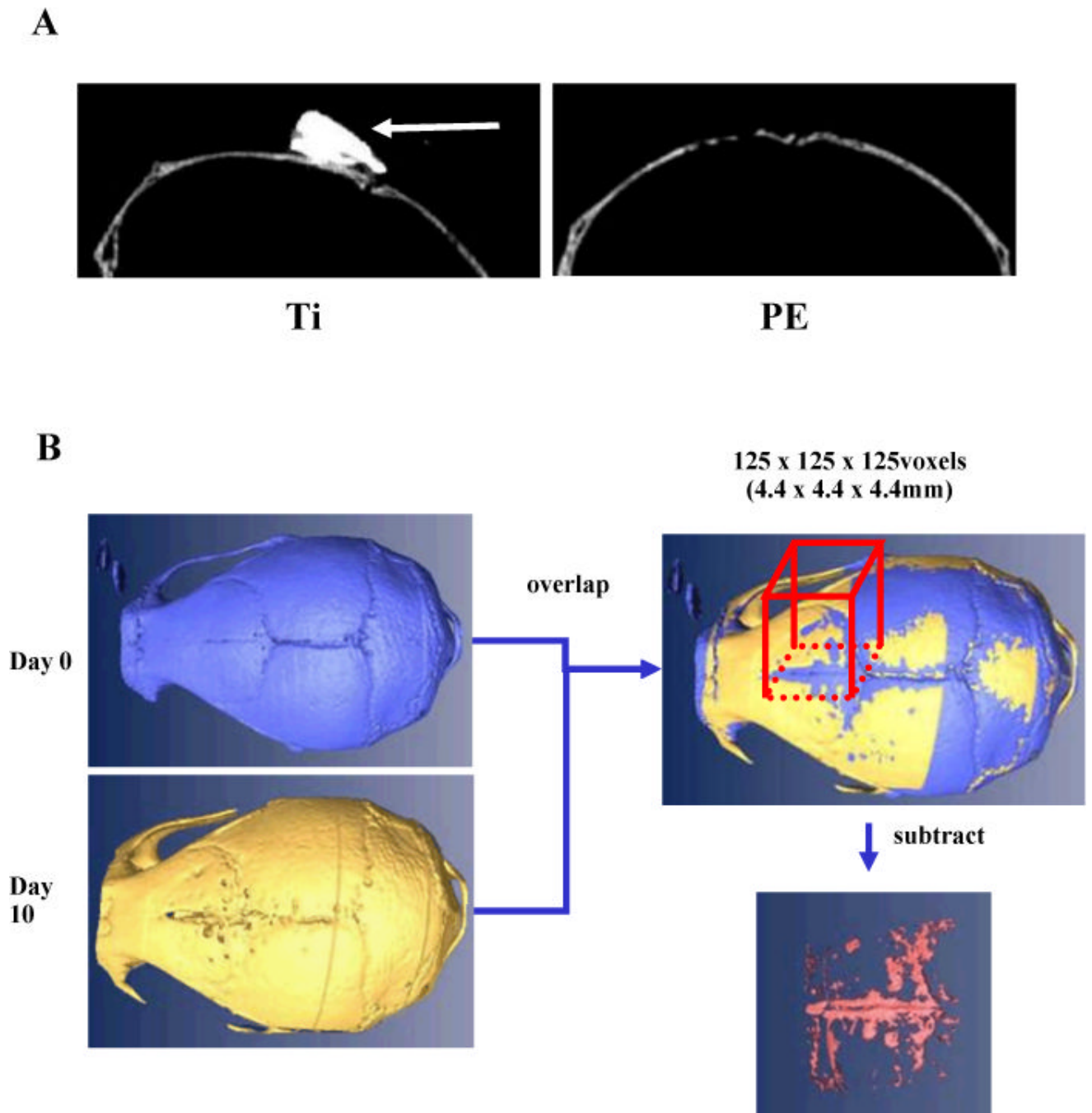


Figure 2. Development of 3D Micro-CT quantification of PE-induced osteolysis

2D *in vivo* micro-CT images of calvaria 10 days after implantation of Ti and PE particles (A). Of note is the high signal produced by the Ti particles (arrow), which could not be accurately segmented away from the bone. In contrast, the absence of a Micro-CT signal from the PE particles allows for reconstruction of the bone volume from the day 0 and day 10 scans, and subtraction of the day 10-bone volume from the day 0-bone volume of a defined region of interest to quantify the volume of osteolysis (B).

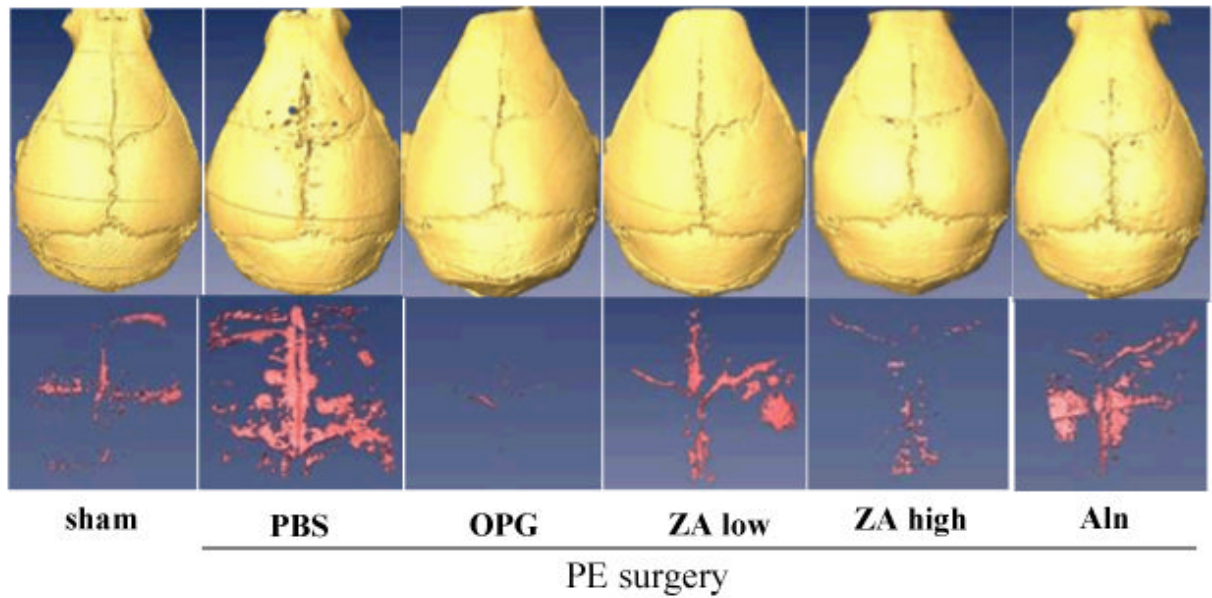
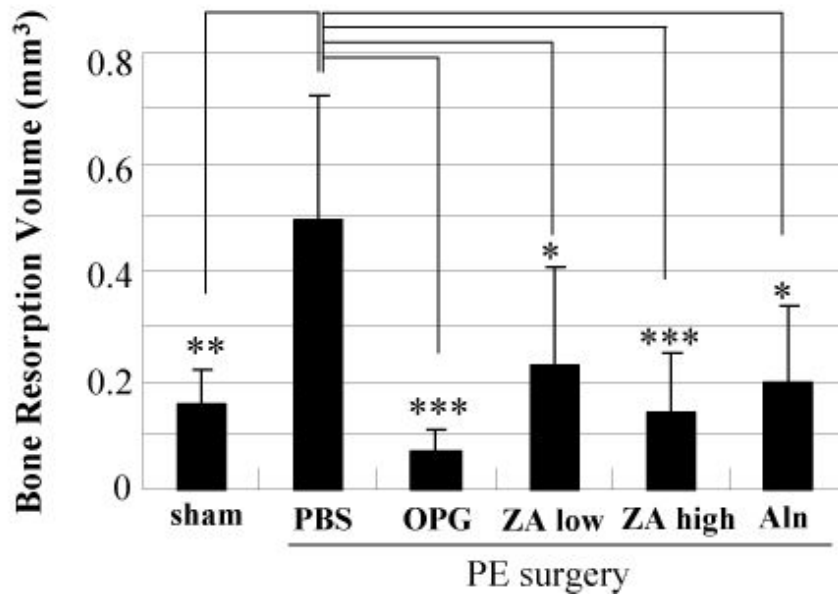
A**B**

Figure 3. OPG vs. BP inhibition of Ceridust-induced osteolysis assessed by longitudinal 3D micro-CT

Mice (n=8) received baseline *in vivo* micro-CT scans before sham or PE surgeries to induce osteolysis over 10 days, and were given PBS, OPG, low dose ZA, high dose ZA or Aln treatment as indicated. Afterwards, the mice received an *in vivo* micro-CT scan to quantify volumetric osteolysis as described in Figure 2. Representative reconstructed images of the calvaria and osteolytic volume from each group are shown (A). The osteolytic volumes from each group are presented as the mean \pm SD (* p<0.05, ** p<0.01, *** p<0.001 vs. PBS control with Tukey test) (B).

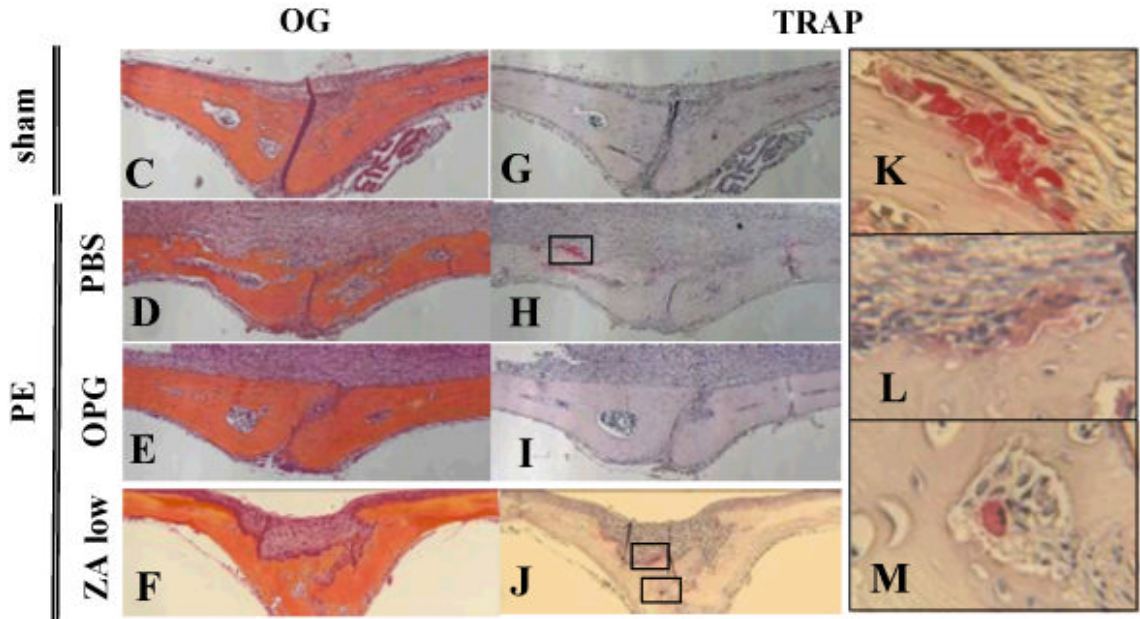
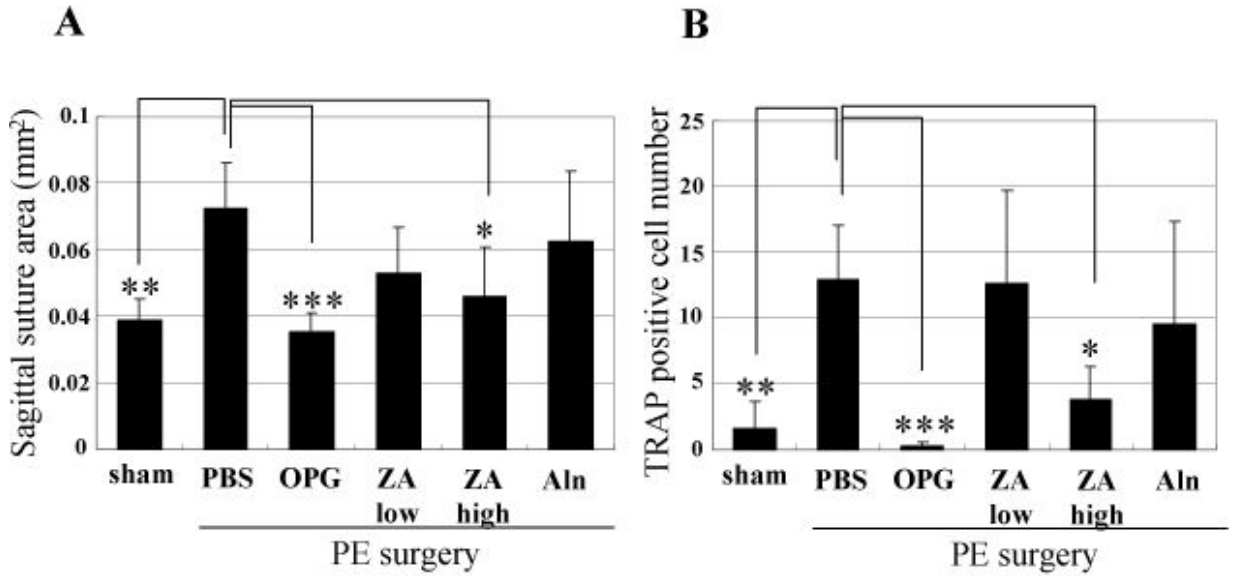


Figure 4. OPG vs. BP inhibition of Ceridust-induced osteolysis assessed by histology

After the day 10 *in vivo* micro-CT scans, the mice described in Figure 3 were sacrificed and their calvaria were harvested for Orange/G and TRAP stained histology to quantify the SSA (A) and osteoclast numbers (B) as described in Figure 1. The data are presented as the mean \pm SD (* $p < 0.05$, ** $p < 0.01$, *** $p < 0.001$ vs. PBS control in Tukey test). Representative Orange/G (C-F) and TRAP (G-M) stained histology are presented at 100X (C-J). High power images of the boxed regions in H and J are also shown at 400X (K-M). Of note are the large number of active osteoclasts in the PBS group (H & K), the complete absence of osteoclasts in the OPG group (I) and the presence of both active (L) and apoptotic (M) osteoclasts in the low dose ZA group.

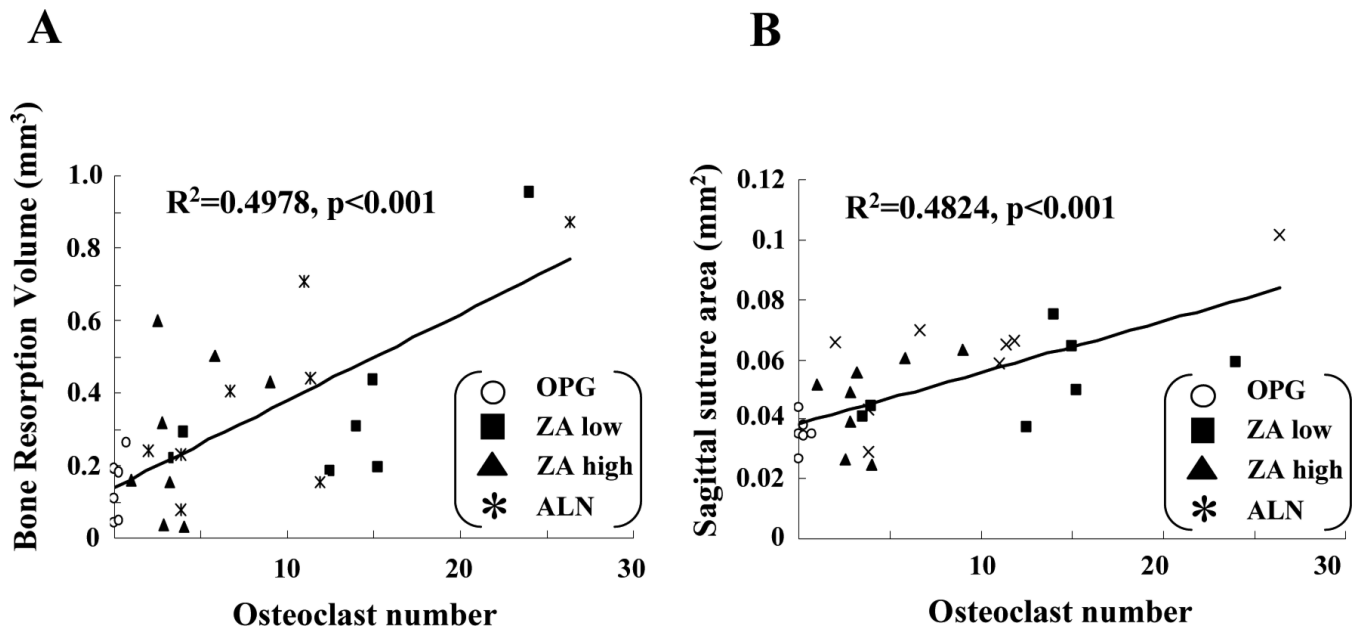


Figure 5. Differences in osteolysis between OPG vs. BP treated mice correlate with osteoclast number

Linear regression analyses were performed to assess the relationship between osteolysis determined by 3D micro-CT in Figure 3B (A) and 2D histomorphometry in Figure 4A (B), versus the number of osteoclasts in Figure 4B.